THE ASTROPHYSICAL JOURNAL, 340:426–434, 1989 May 1

ANALYSIS OF THE NEUTRINO EVENTS FROM SUPERNOVA 1987A

JAMES M. LATTIMER AND A. YAHIL
Astronomy Program, State University of New York at Stony Brook
Received 1988 July 25; accepted 1988 October 14

ABSTRACT

Neutrinos observed from SN 1987A by the Kamioka and IMB detectors are interpreted in terms of thermal emission from a cooling proto–neutron star. This star is the residue of the gravitational collapse of the core of a massive star at the end of its life. It has been shown that the time scale and energy of the neutrino burst is in accord with this scenario. Using both moment and maximum-likelihood methods, the average temperature of the emitted antineutrinos is inferred to be 3–5 MeV, and the total energy emitted in electron antineutrinos is estimated to be $5 \pm 2 \times 10^{52}$ ergs. However, 1 σ errors for the temperature and total energy determinations are large, due primarily to counting statistics. Care has been taken to include the detector response function, which improves, marginally, the agreement between the two detections we analyzed. Also investigated was the statistical significance of the so-called gaps in the arrival times of the neutrinos, especially in the Kamioka data. It is argued that these gaps are due to low counting statistics and not to any pulsing or bursting behavior of the source.

Subject headings: neutrinos — stars: individual (SN 1987A) — stars: supernovae

I. INTRODUCTION

It has long been known that neutrino emission dominates the last phases of the evolution of massive stars (Chiu 1964) and reaches its peak during and after core collapse, when a neutron star, or a black hole, is formed. Such a core collapse is thought to be the mechanism for generating type II supernovae in massive stars (Colgate and White 1966). However, the supernova energy $\sim 10^{51}$ ergs is only a small fraction of the total energy, which is mainly released in the form of neutrinos. In the case of a 1–1.5 $M_\odot$ neutron star, the binding energy which is released is $1.5–3 \times 10^{53}$ ergs. Recent theoretical work on supernovae has shown that the bulk of the neutrinos are emitted over a *multisecond* period as *thermal* neutrino pairs, with a temperature on the order of a few Mev, and with roughly equal numbers of electron, muon, and tau neutrinos (Burrows and Lattimer 1986; Bruenn 1987; Mayle and Wilson 1987).

A proto–neutron star is, to a good approximation, in hydrostatic equilibrium, and the neutrino emission from it occurs in two phases (Burrows and Lattimer 1986). The initial emission is dominated by the cooling and neutronization of the outer, shocked collapsed core, and by matter accreted through the shock and falling onto the hydrostatic residue. This emission lasts perhaps half a second, but contains a substantial fraction, one-third or more, of the total energy. (This phase should not be confused with the "neutronization burst" expected to accompany the breakout of the shock through the neutrinosphere a few milliseconds after the core's bounce. The energy of this burst is only $\sim 1–2 \times 10^{51}$ ergs.) It blends into the long-term diffusion from the inner core. The bulk of the neutrinos in the inner core of the proto–neutron star are ν_e's and have an average energy near 200 MeV. As they diffuse to the surface, their degeneracy energy is converted into heat, resulting in thermal production of ν-$\bar{\nu}$ pairs of all types (Burrows, Mazurek, and Lattimer 1981). Additional paris are created in the hot, shocked, matter at the inner core's edge (Mayle, Wilson, and Schramm 1987). By the time neutrinos are finally emitted from the neutrinosphere, their energies range from 10 to 20 MeV. The long-term emission time scale is primarily determined by the opacity of dense matter (Burrows, Mazurek, and Lattimer 1981; Sawyer and Soni 1979). It is uncertain by at least a factor of 3. The standard model thus predicts that neutrinos of all species should carry away the binding energy in roughly equal amounts. It is expected that $\bar{\nu}_e$'s, because of their large absorption cross section on protons, will dominate the signal in water Čerenkov detectors.

The gross theoretical predictions were dramatically confirmed by the simultaneous observation of a neutrino burst from SN 1987A by the Kamioka (Hirata *et al.* 1987), IMB (Bionta *et al.* 1987), and Baksan (Alekseev *et al.* 1987) experiments. The eight IMB neutrino events, of average energy 34 MeV, spread over 5.6 s, and the 11 Kamioka events (17 MeV, 12.5 s) are clearly in broad agreement with theory.

The purpose of this paper is to analyze in detail what can, and also what *cannot*, be learned about the supernova from the observed events. A statistical analysis of the observed neutrino spectra is performed in § II, resulting in estimates of the average temperature and total energy of the neutrinos. These are compared to similar analyses of other workers, and also to some recent simulations of neutron star formation and cooling. In § III we turn to Monte Carlo simulations of the time behavior of the neutrino events, to investigate the statistical significance of the "gaps" observed in the neutrino data. Conclusions are presented in § IV.

II. SPECTRAL ANALYSIS

The uncertainties in supernova theories, and the small number of observed neutrinos, which are supposed to confront these theories, make it desirable to characterize the spectrum and its time development in some simple parametric form. The analysis of arrival times is deferred to § III. Here we analyze the time-averaged spectrum, which we assume to be Fermi-Dirac, with (average) temperature, T,[1] and zero chemical potential. This is a good assumption for the case of a cooling neutron star (Myra, Lattimer, and Yahil 1987). The data are anyway too meager to allow more spectral parameters to be

[1] Neutrino energies and temperatures are always expressed in Mev.

fitted; the addition of a nonzero chemical potential parameter neither significantly improves the fits to the data, nor changes our estimates for the average temperature and total emitted energy. We discuss this below.

It has been claimed (Bludman and Schinder 1988) that allowing for some time dependence in the cooling and in the neutrino fluxes significantly improves the likelihood of model fits. Incorporating such a time dependence has the effect of increasing the inferred total energy. We will return to these points later.

The published data (Hirata *et al.* 1987, Bionta *et al.* 1987) that we use consist of detection times and estimated electron energies and angles with respect to the Large Magellanic Cloud. It is not possible, except in a statistical sense, to determine which events are due to ν scattering and which to $\bar{\nu}_e$ absorption on protons. The distribution of angles suggests that all but at most one or two of the detections were absorptions. Since theoretical expectations are that less than 5% of the events were due to scattering (e.g., Schramm 1988), we assume here that none were. Our conclusions are not sensitive to this assumption.

For the assumed spectrum, the differential energy distribution function of the neutrinos incident on the detector is proportional to $\epsilon^2 f(\epsilon/T)$, where $f(\epsilon/T) = [1 + \exp(\epsilon/T)]^{-1}$ is the Fermi distribution, and T is the effective temperature. Because the energies and temperature we are interested in are those observed at the Earth, there is no need to include redshift corrections. Redshift corrections must, however, be included in the simulations discussed in the previous section and were indeed used there. The average incident neutrino energy is then

$$\langle\epsilon\rangle_{\rm in} = \frac{\int_0^\infty \epsilon^3 f(\epsilon/T)\,d\epsilon}{\int_0^\infty \epsilon^2 f(\epsilon/T)\,d\epsilon} = T\frac{F_3(0)}{F_2(0)} \simeq 3.15T, \quad (1)$$

where the F_i are the standard Fermi integrals.

In order to obtain the energy distribution function of the *detected* neutrino events, the distribution at the source must be multiplied by the neutrino absorption opacity, $\kappa(\epsilon) = \kappa_0 \epsilon_e p_e$, the detector mass, M, and its detection efficiency $W(\epsilon)$. Here, κ_0 is a constant, and ϵ_e and p_e are the electron energy and momentum, respectively. The existence of a detector threshold, H, the energy below which events are rejected as noise, must also be included. In practice, $W(H) \leq 0.5$.

Additional account must be taken of the experimental errors in the determination of the neutrino energy. Let the detector response function $R(\epsilon, x)$ be the differential conditional probability for measuring an observed neutrino energy ϵ, given a true neutrino energy x. (Unless otherwise stated, we henceforth maintain the distinction between the two energies by using ϵ and x to refer only to the observed and true neutrino energies, respectively.) The differential distribution of observed energies is therefore an integral over all possible true neutrino energies,

$$N(\epsilon) \propto \int_H^\infty x^2 f(x/T)\kappa(x)W(\epsilon)R(\epsilon, x)\,dx\,. \quad (2)$$

Kolb, Stebbins, and Turner (1987) have pointed out that, since the combination of opacity, efficiency, and incoming spectrum is a steep function of the energy, the error in the determination of the detected neutrino energy is not evenly distributed among lower and higher energies. Hence, neglect of the detector response results in a systematic bias. The sense of the bias is that observed energies below the median neutrino energy are underestimated, and those above it are overestimated. Thus, it is likely that the true energy of a neutrino event lies closer to the median energy of the distribution. While it is, of course, hopeless to determine the true energy of a single event from the observed energy, a collection of observations can be corrected for this bias.

We take the energies of the detected electrons, as well as the detector masses, thresholds, and efficiencies, from the discovery papers (Hirata *et al.* 1987; Bionta *et al.* 1987; recent updates, e.g., Matthews 1988, do not affect our conclusions, although the decrease in the energy error bars for the IMB experiment reduces somewhat our quoted errors). The neutrino energies can be determined from the electron energies and angles with respect to the direction of the supernova (Kolb *et al.* 1987); we use the values listed in their Tables 1–2.

The IMB detector is characterized by a threshold energy of $\sim$20 MeV, as compared to 7 MeV for the Kamioka detector. The former will thus only sample the high-energy tail of the spectrum and will provide estimates of somewhat lower reliability. It is interesting that since the characteristics of these detectors are so different, a determination of the temperature can easily be made on this basis (see below).

The errors in the observed energies are reported in the above references to be Gaussian, so the response function can be written as

$$R(\epsilon, x) = \frac{1}{\sqrt{2\pi}\,\Delta} e^{-(\epsilon - x)^2/2\Delta^2}\,, \quad (3)$$

where Δ is the observed error. We have fitted the reported neutrino energies and their errors to determine the following empirical error functions (in mega electron volts):

$$\Delta(\epsilon) = \begin{cases} 0.20 + 0.19\epsilon & \text{Kamioka} \\ -0.38 + 0.26\epsilon & \text{IMB} \end{cases}. \quad (4)$$

In order to assess the importance of the detector response bias, we have also considered the limit of negligible errors, in which the response function becomes a δ-function, and there is effectively no integral in equation (2).

Two general methods are used to analyze the spectrum. The so-called moment method uses only the average energy of the detected neutrinos to determine the temperature, and their number to estimate the total neutrino energy of the supernova. It is alternatively possible to use the mean square energy (the second moment) rather than the mean energy, or even higher moments. We find that this has rather small effect on the results. The maximum-likelihood method, on the other hand, employs the individual energies of the events in the estimate of the temperature, and should, therefore, be more reliable. In fact, both approaches give nearly identical results.

The moment method requires an evaluation of the average detected neutrino energy, obtained by the integration of equation (2) over the observed energy ϵ. At this juncture, we use the standard approximation of treating both W and Δ as functions of x instead of ϵ. Then, the integrated response function, and its first moment, become

$$\int_H^\infty R(\epsilon, x)d\epsilon \equiv A(x) = P\left(\frac{x - H}{\Delta}\right); \quad (5)$$

$$\int_H^\infty \epsilon R(\epsilon, x)\,d\epsilon \equiv xB(x) = xP\left(\frac{x - H}{\Delta}\right) + \Delta^2 R(x, H)\,. \quad (6)$$

Here $P(z) = [1 + \text{erf}\,(z/2^{1/2})]/2$ is the cumulative normal dis-

tribution function. Equations (5) and (6) serve to define the functions A and B, which in the limit of negligible errors, are simply step functions: zero for $x < H$, unity for $x \geq H$. The average detected energy is thus

$$\langle \epsilon \rangle_d = \frac{\int_0^\infty x^3 f(x/T)\kappa(x)W(x)B(x)\,dx}{\int_0^\infty x^2 f(x/T)\kappa(x)W(x)A(x)\,dx} = T\,\frac{G_5(T)}{G_4(T)}\,. \quad (7)$$

We find it useful to refer separately to the integrals in the numerator and denominator of equation (7), which we denote by $G_5 T^6$ and $G_4 T^5$, respectively. They may be viewed as modified, truncated Fermi integrals. (The notation becomes obvious when we recall that κ is essentially proportional to x^2.) Thus the rate of energy absorption by the detector is proportional to $G_5 T^6$, while the detection rate of neutrinos is proportional to $G_4 T^5$. In the limit that the efficiency W is unity, the electron-neutrino energy difference can be ignored, and the observational errors are negligible, the ratio $G_5/G_4 \simeq F_5/F_4 \simeq 5$, and the determination of the temperature from equation (7) is trivial. In general, G_5/G_4 is a function of T, and equation (7) must be solved implicitly for T. A plot of $\langle \epsilon \rangle_d$ versus T, for both detectors, is shown in Figure 1.

In the maximum-likelihood method, one uses the entire energy distribution function $N(\epsilon)$, given by equation (2). In this method, one maximizes the likelihood function, or equivalently minimizes the quantity

$$\Lambda = -2 \sum_{i=1}^{n} \ln N(\epsilon_i)\,, \quad (8)$$

where n is the number of events, with respect to the fitted parameters, in this case T. The minimum value of Λ is arbitrary, but the deviations from the minimum follow the usual χ^2 distribution law, thus allowing error estimates in the usual way (e.g., Kendall and Stuart 1973).

Note that the maximum-likelihood method requires the normalization constant in equation (2) to be set so that the total count is independent of the fitted parameters. Thus, as in the moment method, only shape parameters of the spectrum, i.e., T, can be determined, but not the overall flux. We set the normalization integral to $\int_H^\infty N(\epsilon)\,d\epsilon = n$. For simultaneous fits to both detectors, the sum of the two integrals of the two detectors is set to the total count. The fit is therefore sensitive to the *relative* counts in the two detectors but not to the total number of neutrinos observed.

Once the temperature of the spectrum is determined, the total emitted $\bar{\nu}_e$ energy can be calculated:

$$E_{\bar{\nu}_e} = \frac{4\pi D^2 n F_3(0)}{N_p \kappa_0 G_4 T} = 78.5 \times 10^{51} \left(\frac{D}{50\ \mathrm{kpc}}\right)^2 \frac{F_3(0)}{G_4}\,\frac{n}{MT}\ \mathrm{ergs}\,. \quad (9)$$

Here, D is the distance to the supernova and N_p is the number of protons in the detector. We have $N_p = 6.7 \times 10^{31}\ M$ for an H_2O detector of mass M, in kilotons. We use the value $\kappa_0 = 9 \times 10^{-44}\ \mathrm{cm}^2/\mathrm{proton}$.

Characterizing the neutrino spectrum by a finite chemical potential does not significantly affect the results from equations (1), (7), or (9). In the cases of interest, the integrands of F_i and G_i peak near the energy $x \simeq iT$. Thus, the 1 in the Fermi factor f becomes negligible compared to the exponential for small or moderate chemical potential μ, and we may write $f \simeq e^{(\mu - x)/T}$. The term $e^{\mu/T}$ is thus common to all such integrals. In equations (1), (7), and (9) these terms cancel, leaving essentially no μ dependence. On the other hand, if one were to attempt to derive a neutrinosphere radius R from the relation $E_{\bar{\nu}_e} \propto 4\pi R^2 F_3 T^4$ (Spergel *et al.* 1987; Lamb, Melia, and Loredo 1988), the unbalanced chemical potential factor in F_3 renders the result very sensitive to the assumed value of μ/T. For example, compared to the case of zero chemical potential, if μ/T were 1(3), the derived radius is smaller by a factor of 0.63 (0.27). It is therefore difficult to extract reliable information on the radius of the emitting surface in the case of SN 1987A.

Some results for these approaches are presented in Table 1 and in Figures 2 and 3. It is seen that the temperatures in Table

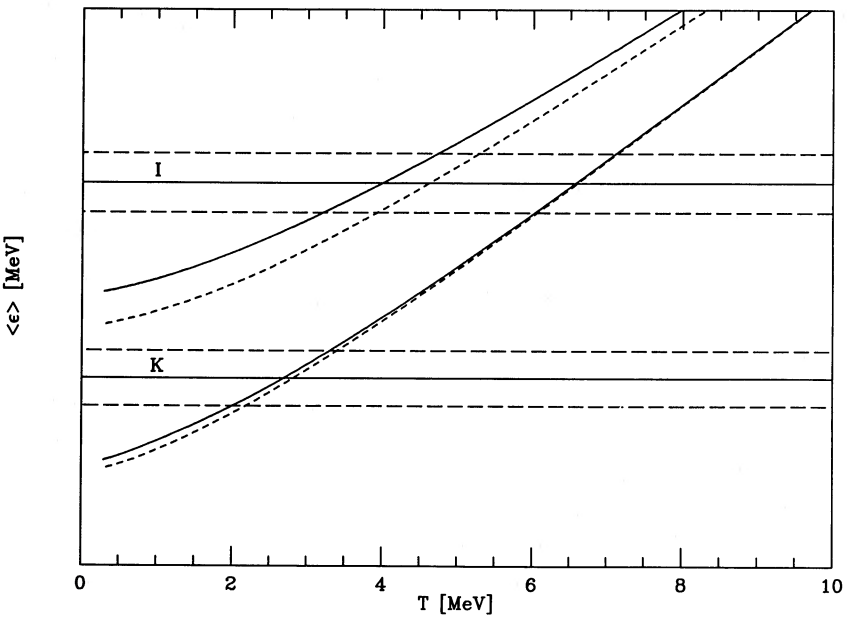

FIG. 1.—Average detected neutrino energy as a function of neutrino temperature from the moment method. K refers to Kamioka, I to IMB. Solid curves include detector response (*see text*); dashed curves do not. Solid horizontal lines are the observed values, and dashed lines are 1 σ deviations.

TABLE 1

DERIVED TEMPERATURES (MeV) AND TOTAL ENERGIES (10^{51} ergs)

Method of Analysis	$T_{\rm Kamioka}$	$T_{\rm IMB}$	$E_{\rm Kamioka}$	$E_{\rm IMB}$
Without Detector Response				
Moment	2.8 ± 0.6	4.6 ± 0.8	61^{+50}_{-30}	29^{+26}_{-16}
Maximum-likelihood	2.8 ± 0.4	4.7 ± 0.8	59^{+34}_{-28}	27^{+26}_{-10}
Maximum-likelihood (combined)	3.8 ± 0.4		43^{+20}_{-18}	
With Detector Response				
Moment	2.8 ± 0.5	4.0 ± 0.7	69^{+55}_{-38}	57^{+100}_{-28}
Maximum-likelihood	2.8 ± 0.4	4.2 ± 1.0	63^{+40}_{-31}	45^{+120}_{-34}
Maximum-likelihood (combined)	3.7 ± 0.4		48^{+21}_{-18}	
Relative counts	$5.0^{+1.25}_{-1.0}$		26^{+19}_{-16}	

1 derived from the two detections differ by a factor of 1.5, although this is not statistically significant (within 1 σ). Considering the simplicity of the assumptions, this is comforting. What is surprising is that the two methods give nearly identical results for each experiment. We find that more complex, e.g., time-dependent, spectra do not give better fits to the observed neutrino energies. The basic problem is low counting statistics, which frustrates multiparameter fits.

For comparison, in the case of negligible errors and unity efficiency, we would have $T \simeq \langle \epsilon \rangle_d/5$. For Kamioka and IMB, this would imply temperatures of 3.3 and 6.7 MeV, respectively. The total $\bar{\nu}_e$ energy would be $E_{\bar{\nu}_e} \simeq 19.1 \times 10^{51}\ n/MT$ ergs for $D = 50$ kpc, or 30.3 and 4.6×10^{51} ergs, respectively. It is clear that the combinations of efficiency and threshold are more energy dependent for IMB, in that the effective orders of the modified Fermi integrals become larger, and the effective corrections become greater.

Note from equations (5)–(6) that for a finite observed error Δ, $A(x) < B(x)$. From equation (7) we can therefore deduce that, for a given mean observed neutrino energy, including the detector response results in a decrease of the estimated temperature. It similarly follows from equation (9) that the estimated total emitted energy increases. Because the IMB ν's lie in the tail of the Fermi distribution, beyond the peak in the spectrum, the effect of detector response is much greater for the IMB detector. Therefore, the IMB and Kamioka temperatures and, in particular, the total energies are pushed even closer together.

The effects of detector response are more easily seen in Figure 2, which displays the total energy per detected neutrino as a function of the average energy. This quantity, $E_{\bar{\nu}_e}/n$, is independent of n, as can easily be seen from equation (9), keeping in mind that T does not depend on n. Results with and without detector response are shown for each detector. Although this figure is drawn from the moment method analysis, it is clear that the maximum-likelihood case is very similar, and Figure 1 can be used to convert one to the other. Clearly, the high threshold energy of the IMB detector makes it depend more sensitively on detector response effects. In addition, note that the one sigma error estimates lead to a rather large uncertainty in the determination of the total energy whether or not detector response is included. Figure 3 displays $E_{\bar{\nu}_e}$ as a function of the temperature and n, in the maximum likelihood method, for the (*a*) Kamioka and (*b*) IMB data.

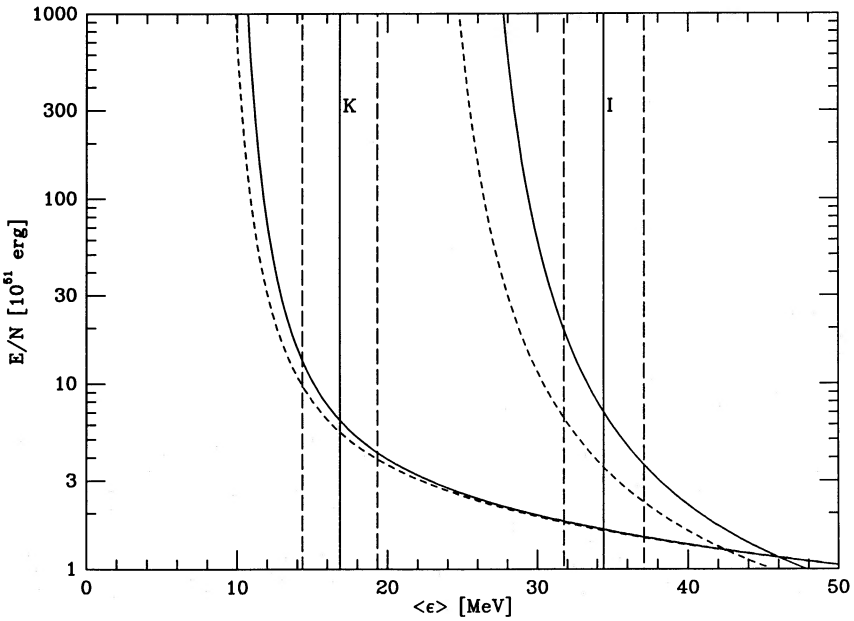

FIG. 2.—Inferred total $\bar{\nu}_e$ energy per detected neutrino in units of 10^{51} ergs as a function of the average detection energy. The notation is the same as in Fig. 1, except that the vertical lines refer to observed values and 1 σ deviations.

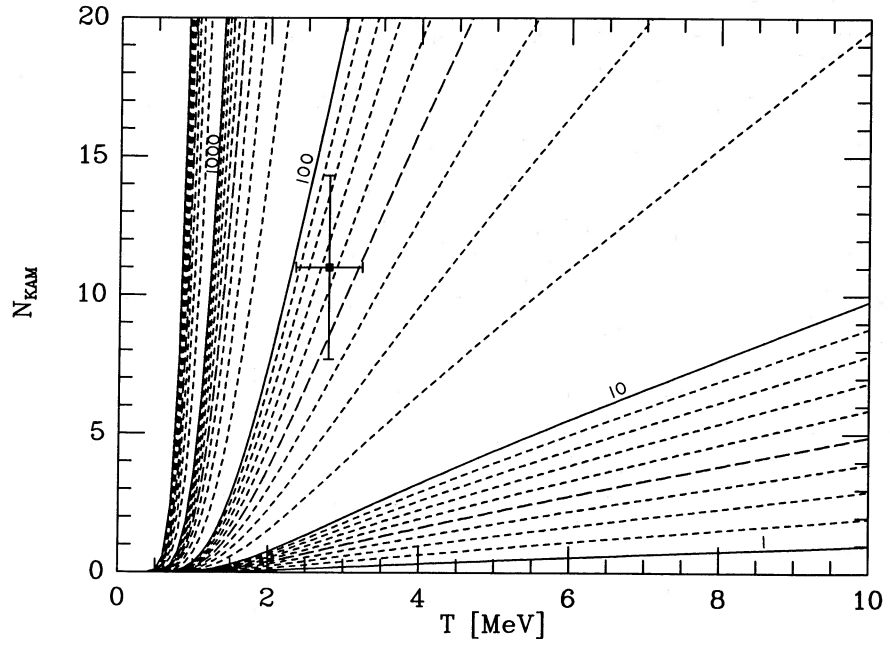

FIG. 3*a*

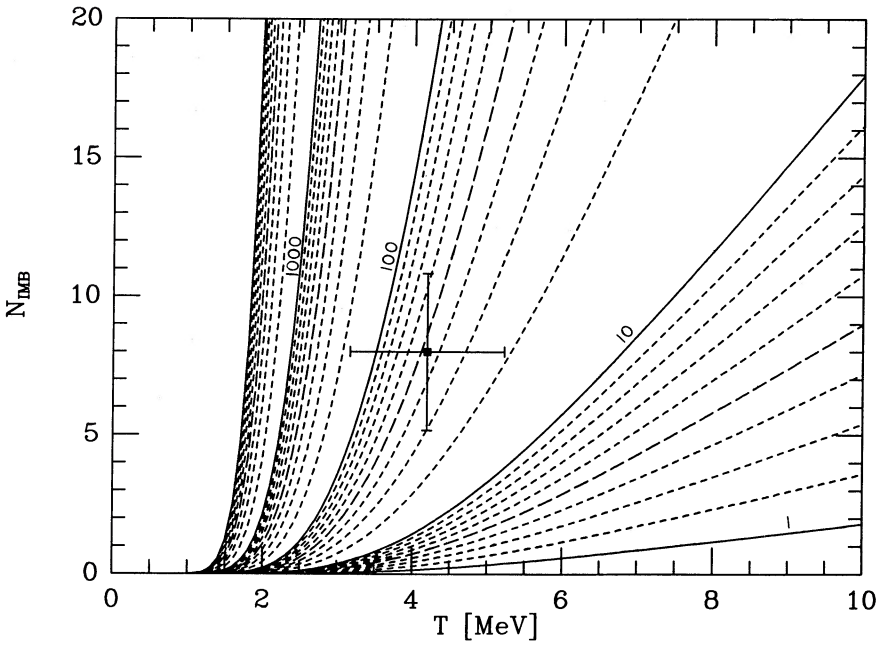

FIG. 3*b*

FIG. 3.—Contours of the total energy, in units of 10^{51} ergs, as a function of the number of detected neutrinos and the temperature for the (*a*) Kamioka and (*b*) IMB experiments. The squares mark the maximum likelihood fit; error bars are 1 σ (including Poisson counting errors).

It is possible to combine data from both detectors, assuming that they both observed the same event (i.e., the total energies and temperatures were the same). This should result in improved estimates. In the moment method, this is accomplished by examining the ratio of events seen by Kamioka to those seen by IMB. For identical detectors this ratio is, of course, insensitive to the spectrum. Owing to the different detection efficiencies and thresholds, however, it becomes a measure of the neutrino temperature. Specifically, forcing the total energies and temperatures inferred by the two experiments to be equal gives the condition (see eq. [9]) that the quantity $G_4 M/n$ must also be the same for both. Figure 4 shows the temperature as inferred from this condition for the two cases in which the response function is and is not included. Results from this calculation are included in Table 1, and overlap, within the errors, with the other methods.

When the maximum-likelihood method is applied to the combined data, a temperature estimate results which is intermediate between the temperatures derived for each data set separately. By contrast, the temperature deduced from the ratio of counts is in excess of those determined individually from the two detectors, although within their error estimates.

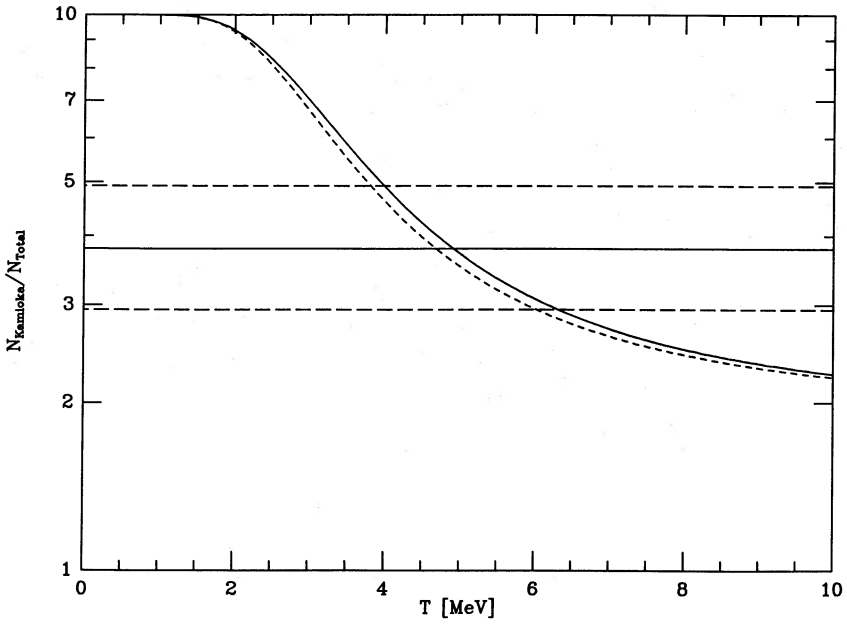

FIG. 4.—The ratio of expected Kamioka counts to Kamioka plus IMB counts as a function of temperature. The solid curve includes detector response, the dashed curve does not. The solid horizontal line is the observed ratio and the dashed lines represent 1 σ errors.

This behavior underscores the higher reliability of maximum-likelihood estimates, which probe the entire probability distribution, and hence all its moments, in contrast with moment methods, which are sensitive to only a ratio of two moments.

When one attempts to determine the total energy of the supernova, the Poisson uncertainties associated with the number of detected neutrinos must be added to those in the temperature estimates. This is illustrated in Figure 5, in which contours of $E_{\bar{\nu}_e}$ are plotted as functions of the number of detected neutrinos and (*a*) the temperature derived in the maximum-likelihood fit to the combined data set and (*b*) the ratio of counts in the two detectors. In both cases there are large uncertainties.

Spergel *et al.* (1987) have also analyzed, in a maximum likelihood, constant temperature, model the Kamioka and IMB data, but restricted their study to the first eight Kamioka neutrinos. The temperature they derived, 4.1 MeV, is close to what our analysis would give for the same data. Bludman and Schinder (1988) have obtained 3.7 MeV for this case. For the entire 19 neutrino data set, Bludman and Schinder found 3.3 ± 0.3 MeV. While this temperature estimate lies just 1 σ from ours, we do not understand this difference.

Both Spergel *et al.* and Bludman and Schinder also considered models in which the temperature decayed with time. In the case of exponential decay, these groups found best-fit initial temperatures of 4.2 and 3.8 MeV, respectively, luminosity decay times of 4.5 and 4.8 s, respectively, and $E_{\bar{\nu}_e}$ of 6.1 and 6.7×10^{52} ergs, respectively. (Lamb *et al.* 1988 have also reported very similar results.) Bludman and Schinder further considered a power-law decay, which introduces one additional fitting parameter. In their best-fit power-law case, they find $E_{\bar{\nu}_e} = 9.2 \pm 3.3 \times 10^{52}$ ergs. This marginally significant increase in $E_{\bar{\nu}_e}$ is curious when compared to neutron star formation and cooling simulations (Burrows and Lattimer 1986; Mayle and Wilson 1987) that explicitly calculate the time-varying temperature and luminosity in a consistent fashion. These models fit the observed number of neutrino counts for $E_{\bar{\nu}_e}$ in the range $3\text{–}4 \times 10^{52}$ ergs (Burrows 1988; Mayle and Wilson 1987). These are consistent with that inferred from constant temperature models. The difference cannot be attributed to that fraction of the energy emitted after the last neutrino was detected, which the constant temperature models ignore, because this fraction is small. In the power-law case it is less than 4% of the total.

The resolution of this discrepancy may reside with the overly simple nature of the exponential or power-law cooling, compared to what is expected from physical models. The latter imply an initially rapidly decaying (luminosity time constant ≤ 0.5 s) flux and temperature as the neutron star shrinks from a beginning radius of ~ 100 km to a radius of 20 km. This stage is followed by a slower, quasi-static, cooling phase (time constant $\sim 5\text{–}10$ s). The observations tend to support this interpretation in that about half the counts accumulate within 1 s; compare this to the best-fit exponential models referred to above, in which the 4.5 s decay times imply that it takes 2–2.5 s for half the signal to accumulate. The introduction of a smoothly decaying temperature is equivalent to changing the spectrum from that of a Fermi-Dirac in that the high-energy tail becomes suppressed. As a result, the overall flux must be increased to compensate, which results in an increased total emitted energy. Therefore, surprisingly, the constant temperature models may more accurately portray the energetics of SN 1987A, in which counting statistics are poor.

We conclude this section by noting that the inferred total $\bar{\nu}_e$ energy can be used to estimate the mass of the neutron star that might have formed. According to detailed models of neutrino emission, each of the six known neutrino species carries a nearly equal share of the total energy. Thus, the total binding energy of the neutron star is ~ 6 times $E_{\bar{\nu}_e}$, or $2.5 \pm 1 \times 10^{53}$ ergs. In spite of the relatively large uncertainties in the equation of state above nuclear densities, the binding energy versus gravitational mass relationship for neutron stars is rather well determined. We show this relation in Figure 6, which contains a compendium of models with widely varying stiffnesses

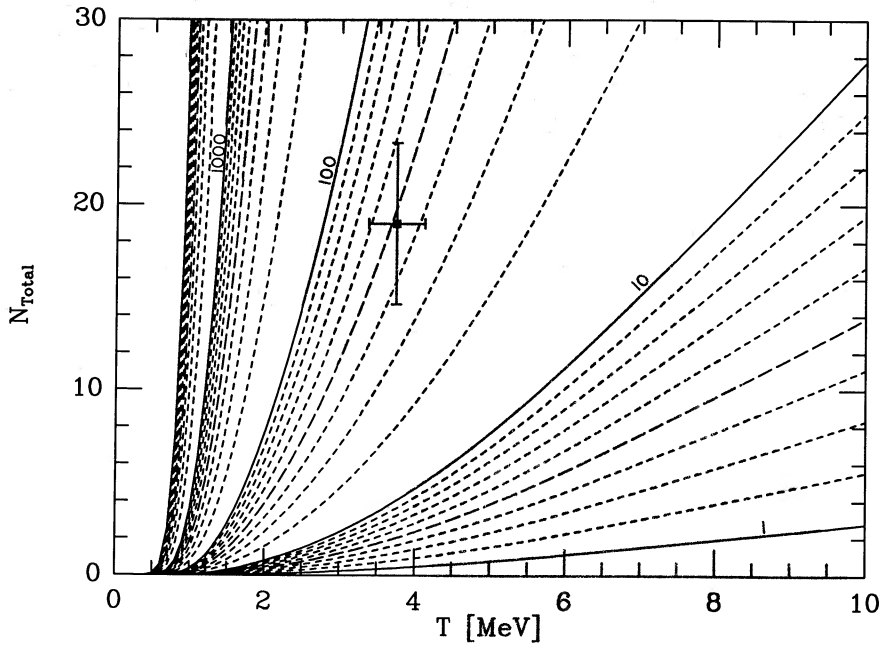

FIG. 5a

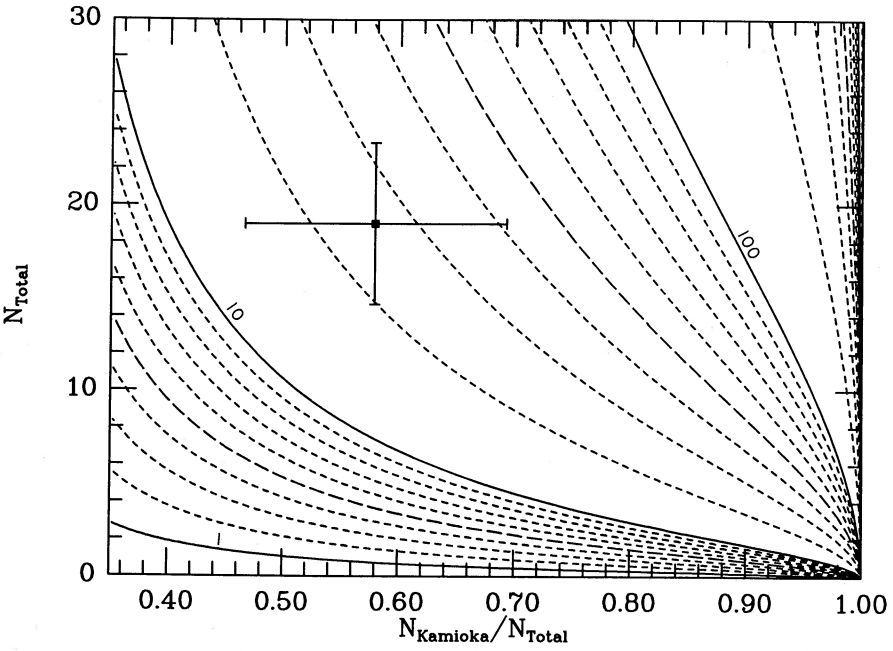

FIG. 5b

FIG. 5.—Contours of total $\bar{\nu}_e$ energy, in units of 10^{51} ergs, as a function of the total number of detected events and (*a*) the temperature estimate from the maximum-likelihood fit to the combined data set, and (b) the ratio of counts (from the moment method) from the two detectors. The squares mark the best fit and the error bars are 1 σ (including Poisson errors).

(Glendenning 1988*a*,*b*; Prakash, Ainsworth, and Lattimer 1988). The role of differences between equations of state is limited to the determination of the neutron star's maximum mass and binding energy, at least for stars more massive than one solar mass. While the true stiffness of an equation of state is ultimately measured by its value for the neutron star's maximum mass, one quantity that is often referred to is the bulk compression modulus of nuclear matter. In Figure 6, the equations of state compared have compression moduli ranging from 60 to 300 MeV, which encompasses most recent experimental and theoretical estimates. Nevertheless, the spread in binding energies, for a given gravitational mass, is only $\sim 15\%$. For $M > 1\ M_\odot$, an acceptable fit is given by

$$E = 1.5 \times 10^{53} \left(\frac{M}{M_\odot} \right)^2 \text{ ergs} , \qquad (10)$$

where M is the neutron star's gravitational mass. The above

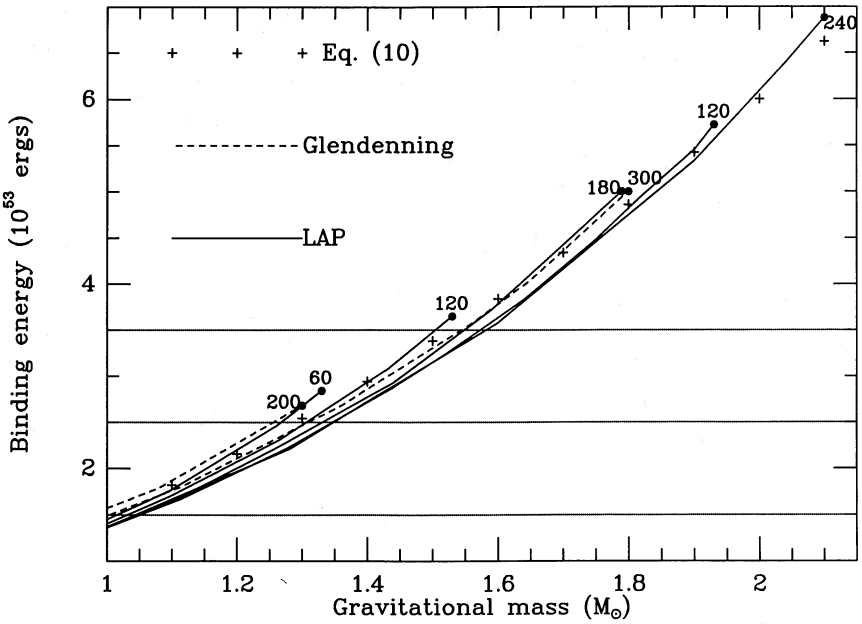

FIG. 6.—Binding energy vs. neutron star mass from a variety of equations of state (*see text*). Each is labeled by that equation of state's nuclear matter compression modulus, in MeV, and ends in a dot which marks the maximum mass configuration. Plus signs show an approximate fit (eq.[10]).

energy thus translates into neutron star gravitational masses in the range 1.0–1.6 $M_\odot$. It is difficult to determine from the energetics alone the mass and, therefore, which explosion mechanism might have occurred in the case of SN 1987A.

III. ANALYSIS OF ARRIVAL TIMES

Many authors have commented on the bunched structure that the Kamioka data show in the arrival times. It has prompted some to conclude the distribution is inconsistent with that predicted by a simple cooling model, namely, an exponential or power-law signal decay, and instead to propose a variety of explanations for this behavior. Without detailing the list of ideas, which range from pion condensates and quark-baryon phase transitions, through rapid rotational breakup and reaccretion scenarios, to secondary collapses to black holes, we feel motivated to determine just how likely the observed structure might be. We will concentrate on the Kamioka data alone, although it is well worth pointing out that the last few IMB events fill in the largest gap in the Kamioka data, and probably render this entire discussion academic.

Based on the ability of straightforward models of neutron star cooling to give the right number of counts, the right average energy, and the correct time scales over which neutrino emission occurs, it seems sensible to test the significance of gaps by simple parametrizations of such models. Another approach is to fit a smooth curve through the observations themselves. Choosing a model for the signal accumulation, one can then perform a series of Monte Carlo simulations with a Poisson distribution of total counts about a mean, and simply ask: what is the probability that a gap will occur that is longer than Δt seconds, and has a certain number of neutrinos coming after it?

We have used two model functions: first, a smooth curve fitted to the data (it was not required to pass through the data points), and second, a double exponential decay model that fits both the data and models of neutron star cooling. For the latter, the signal accumulation rate is

$$\frac{dN}{dt} \propto e^{-t/t_1} + \frac{t_1}{t_2} e^{-t/t_2}, \tag{11}$$

where $t_1 \simeq 0.5$ s and $t_2 \simeq 6$ s. The adopted form of this equation has the property that both time scales contribute equally to the integrated signal. The two time scales correspond to the two phases of ν emission discussed previously.

Results are shown in Figure 7. We interpret them as follows: the situation of having a gap of 7 s duration, with at least three neutrinos following the gap, occurs $\sim 5\%$ of the time. This result *is* sensitive to the functional form of the signal accumulation. Functions that have a much greater or much smaller amount of accumulation at late times ($t > 10$ s) will result in correspondingly higher or lower probabilities of having lengthy gaps in the data. The point made here is that reasonable signal accumulation functions, which adequately fit the data, have acceptable probabilities for showing a gap in an observation with a small number of detections.

Before we decide that this gap is even marginally significant, however, two additional questions need to be asked. First, if the gap is real, how can we understand the absence of a gap in the IMB data? Secondly, would a gap of the same duration, but having only two trailing neutrinos, or a gap of, say, 5 s duration with three trailing neutrinos, have elicited the same response (i.e., number of preprints)? We think that the IMB data can not easily be reconciled with a real gap, and that a gap, whose probability under the null-hypothesis of no gap was higher than 5%, would not have prevented speculation about its reality. We take the opposite view, and recommend caution. The fact is that small number statistics is at play, and gaps are not uncommon in such data sets.

IV. CONCLUSIONS

Both the maximum-likelihood and the moment analyses of the neutrino observations from SN 1987A show that the

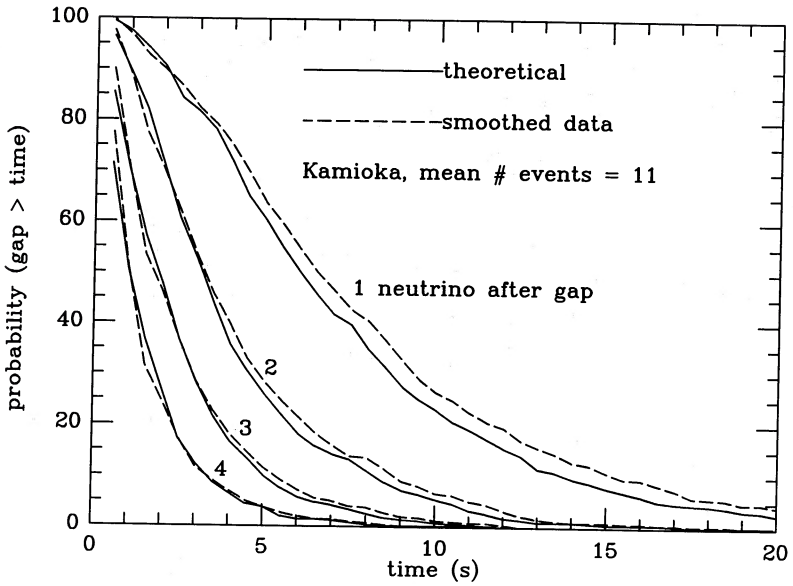

FIG. 7.—Probabilities that gaps with duration larger than t seconds and with the labeled number of trailing neutrino events occur in randomly generated data sets which have a Poisson mean of 11 events. The parent signal accumulation function follows eq. (11) for the solid curves, and a smoothed fit to the Kamioka observations for the dashed curves.

received spectrum was consistent with being thermal with an average temperature 3–5 MeV, and that a total energy of $5 \pm 2 \times 10^{52}$ ergs in electron antineutrinos was emitted. The importance of including the detector response function was pointed out. Fits incorporating a simple power law or exponential cooling behavior seem to raise this energy estimate by up to a factor of 2. However, neutron star formation and cooling simulations seem to favor constant temperature estimates, because of the two-stage nature of the cooling. The equivalence of the emitted energy with a neutron star's binding energy leads to the conclusion that a 1.0–1.6 $M_\odot$ neutron star was created. (Theoretical simulations of neutron star cooling imply a somewhat smaller range, 1.0–1.4 $M_\odot$.) Statistical analyses of the arrival times of the neutrinos reveals that the observed bunches and gaps are what can be reasonably expected from the standard neutron star cooling scenario. Some recent statements to the contrary are probably due to *a posteriori* statistics.

We appreciate conversations with E. Beier, G. E. Brown, A. Burrows, J. Cooperstein, S. Kahana, A. Mann, and E. Myra. This research was supported in part by USDOE grant DE-FG02-87ER40317.A000.

REFERENCES

Alekseev, E. N., Alekseeva, L. N., Volchenko, V. I., and Krivosheina, I. V. 1987, *Soviet Phys.—JETP Letters.*, **45**, 589.
Bionta, R. M., *et al.* 1987, *Phys. Rev. Letters*, **58**, 1494.
Bludman, S. A., and Schinder, P. J. 1988, *Ap. J.*, **326**, 265.
Bruenn, S. A. 1987, *Phys. Rev. Letters*, **59**, 938.
Burrows, A., and Lattimer, J. M. 1986, *Ap. J.*, **307**, 178.
Burrows, A., Mazurek, T. J., and Lattimer, J. M. 1981, *Ap. J.*, **251**, 325.
Chiu, H. Y. 1964, *Ann. Phys.*, **26**, 364.
Colgate, S. A., and White, R. H. 1966, *Ap. J.*, **143**, 626.
Glendenning, N. K. 1988*a*, *Nucl. Phys.*, **A480**, 597.
———. 1988*b*, LBL preprint 25032.
Hirata, K., *et al.* 1987, *Phys. Rev. Letters*, **58**, 1490.
Kendall, M. G., and Stuart, A. 1973, *The Advanced Theory of Statistics*, Vol. **2** (New York: Hafner).
Kolb, E. W., Stebbins, A. J., and Turner, M. S. 1987, *Phys. Rev., D*, **35**, 3598.
Lamb, D. Q., Melia, F., and Loredo, T. J. 1988, in *Supernova 1987A in the Large Magellanic Cloud*, ed. M. Kafatos and A. Michalitsianos (Cambridge: Cambridge University Press), p. 204.
Matthews, J. 1988, in *Supernova 1987A in the Large Magellanic Cloud*, ed. M. Kafatos and A. Michalitsianos (Cambridge: Cambridge University Press), p. 151.
Mayle, R., and Wilson, J. R. 1987, Livermore preprint UCRL-97355.
Mayle, R., Wilson, J. R., and Schramm, D. N. 1987, *Ap. J.*, **318**, 288.
Myra, E. S., Lattimer, J. M., and Yahil, A., in *Supernova 1987A in the Large Magellanic Cloud*, ed. M. Kafatos and A. Michalitsianos (Cambridge: Cambridge University Press), p. 213.
Prakash, M., Ainsworth, T. and Lattimer, J. M. 1988, *Phys. Rev. Letters*, **61**, 2518.
Sawyer, R. F., and Soni, A. 1979, *Ap. J.*, **230**, 859.
Schramm, D. N. 1988, in *Proc. 22d Recontre de Moriond*, in press.
Spergel, D. N., Piran, T., Loeb, A., Goodman, J. and Bahcall, J. N. 1987, *Science*, **237**, 1471.

JAMES M. LATTIMER and A. YAHIL: Astronomy Program, State University of New York, Stony Brook, NY 11794-2100